

# The nature of X-ray spectral variability in Seyfert Galaxies

Richard D. Taylor<sup>\*</sup>, Philip Uttley and Ian M. M<sup>c</sup>Hardy

*Department of Physics and Astronomy, University of Southampton, Southampton, SO17 1BJ*

Received \*\* \*\* 2003 / Accepted \*\* \*\* 200\*

## ABSTRACT

We use a model-independent technique to investigate the nature of the 2–15 keV X-ray spectral variability in four Seyfert galaxies and distinguish between spectral pivoting and the two-component model for spectral variability. Our analysis reveals conclusively that the softening of the X-ray continuum with increasing flux in MCG–6-30-15 and NGC 3516 is a result of summing two spectral components: a soft varying component (SVC) with spectral shape independent of flux and a constant hard component (HCC). In contrast, the spectral variability in NGC 4051 can be well described by simple pivoting of one component, together with an additional hard constant component. The spectral variability model for NGC 5506 is ambiguous, due to the smaller range of fluxes sampled by the data. We investigate the shape of the hard spectral component in MCG–6-30-15 and find that it appears similar to a pure reflection spectrum, but requires a large reflected fraction ( $R > 3$ ). We briefly discuss physical interpretations of the different modes of spectral variability.

**Key words:** Galaxies: individual: MCG–6-30-15 - X-rays: galaxies - Galaxies: Seyferts - galaxies: active

## 1 INTRODUCTION

Rapid X-ray variability is common in Seyfert galaxies (Green et al., 1993) and suggests that the X-ray emission originates close to the central black hole. In a number of Seyfert galaxies, the 2–20 keV continuum spectrum steepens with increasing X-ray flux (Iwasawa et al. 1996; Lamer et al. 2000; Lamer et al. 2003; Lee et al. 2000; Chiang et al. 2000; Done et al. 2000). This softening of the X-ray emission is commonly attributed to a change in shape of a single continuum component, possibly due to the Compton cooling of the X-ray emitting corona by the increased seed photon flux (Haardt et al., 1997).

Recent spectral variability studies of MCG–6-30-15 with *RXTE* (M<sup>c</sup>Hardy et al., 1998) and subsequently with *ASCA* (Shih et al., 2002) have shown that the photon index appears to saturate at high X-ray fluxes. To explain this effect, which Lamer et al. (2003) also observe in NGC 4051, M<sup>c</sup>Hardy et al. (1998) and Shih et al. (2002) independently proposed a two-component spectral model, consisting of a soft component with constant spectral slope but variable flux and a hard component with constant flux, so that at high fluxes the soft component dominates the spectrum and the spectral slope saturates to the slope of the soft component. This model naturally explains the observed spectral variability as a result of the relative changes in flux of the hard and soft continuum components, without recourse to any intrinsic change in the shape of either spectral component. Using time-resolved spectral analysis of a long XMM-Newton observation of MCG-6-30-15, Fabian & Vaughan

(2003) have shown that, on 10 ks time-scales, the X-ray spectral variability of this AGN is accounted for by a two-component model where the soft varying component is a power-law (with roughly constant slope) and the hard constant component is produced by very strong reflection from a relativistic disk. Fabian & Vaughan (2003) suggest that the large amplitude of reflection may be boosted by gravitational light-bending effects close to a Kerr black hole.

As an alternative to the two-component model, Zdziarski et al. (2003) have suggested that the apparent saturation of the photon index at high fluxes may instead be a result of a simple pivoting of the X-ray spectrum about some relatively high energy ( $\sim 60$  keV or greater), so that the photon index increases with the logarithm of the flux. In order to understand the physical implications of spectral variability in Seyfert galaxies, it is important to distinguish between the spectral-pivoting and two-component models. Here, we present a model independent technique which enables us to determine conclusively that the two-component model for spectral variability is correct in the case of MCG–6-30-15 and the Seyfert galaxy NGC 3516, but not in NGC 4051 which shows evidence for pivoting. This technique is outlined in Section 2. The data collection and reduction is described in Section 3. The observational results and the implications for the interpretations of spectral variability in AGN are discussed in Sections 4 and 5.

## 2 METHOD

Consider the total fluxes measured in hard and soft energy bands ( $F_h$  and  $F_s$ , respectively). We can express each flux as the sum of constant ( $C_h$  and  $C_s$ ) and variable ( $f_h$  and  $f_s$ ) components.

\* e-mail: rdt@astro.soton.ac.uk

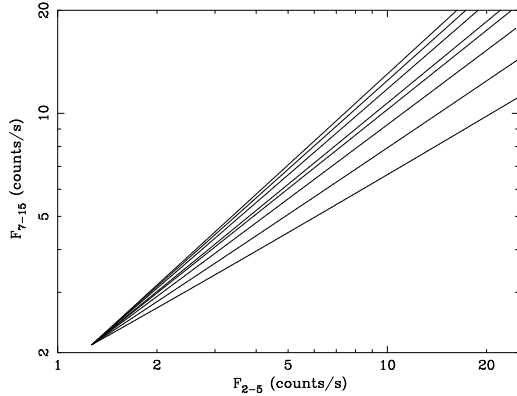


**Figure 1.** Flux-Flux representation of spectral variability as a result of spectral pivoting for a number of pivot energies (from the bottom  $E_p = 30, 100, 300, 1000, 3000, 10000$  keV with  $F_h$  vs  $F_s$  relations described by power-laws with corresponding slopes  $\alpha = 0.56, 0.73, 0.79, 0.83, 0.86, 0.88$ ). The flux-flux relations were simulated using the XSPEC FAKEIT command to create fake *RXTE* spectra, from which the fluxes in each band can be determined.

$$F_s = f_s + C_s \quad (1)$$

$$F_h = f_h + C_h \quad (2)$$

A simple parameterisation of flux-dependent spectral variability relates the hard and soft variable fluxes, by  $f_h = kf_s^\alpha$ , where  $k$  and  $\alpha$  are constants. If  $\alpha < 1$  this relation describes power-law pivoting spectral variability, where the varying power-law pivots about some energy  $E_p$  (larger than the observed energies) while keeping the flux density at  $E_p$  constant (see appendix in Zdziarski et al. 2003, and Fig. 1). As pivot energy increases, so  $\alpha$  asymptotically approaches 1. In the case of  $\alpha = 1$ , the spectral shape of the varying component is constant with a hardness ratio  $k$ . Values of  $\alpha > 1$  correspond to a pivot energy which lies below the soft energy band. Incorporating varying and constant continuum components, we obtain the following relation between  $F_h$  and  $F_s$ :

$$F_h = k(F_s - C_s)^\alpha + C_h \quad (3)$$

By plotting  $F_h$  vs  $F_s$  (which we call a ‘flux-flux plot’), we reveal the nature of the spectral variability. Specifically, if the varying component has constant spectral shape the  $F_h$  vs  $F_s$  relationship will be linear with gradient  $k$  (i.e. the hardness ratio of the varying component), and an intercept  $C = C_h - kC_s$  (this linear form occurs irrespective of the actual spectral shape of the varying component). In contrast, if the spectral shape of the varying component depends on flux the  $F_h$  vs  $F_s$  relationship will not be linear. In particular, if the spectral variability is explained by simple power-law pivoting, with no constant components, the  $F_h$  vs  $F_s$  relationship will be well fitted with a simple power-law. Other non-linear shapes of the  $F_h$  vs  $F_s$  relationship might be envisaged for more complicated forms of spectral variability, or if the varying component spectrum is not a power-law. Note that such an approach has previously been used by Churazov et al. (2001) to show the existence of a constant soft spectral component in the high/soft state spectrum of the black hole X-ray binary Cyg X-1.

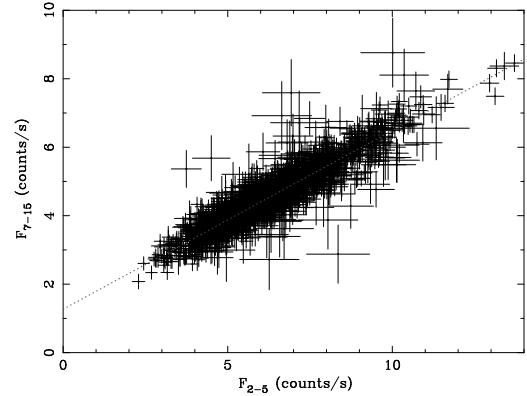


**Figure 2.** The flux-flux plot for MCG-6-30-15 (see text for details). The dashed line represents the linear fit to the data

### 3 OBSERVATIONS AND DATA REDUCTION

In order to test our method, we first use PCA data from *RXTE* observations of MCG-6-30-15 to examine the spectral variability of this source using flux-flux plots. MCG-6-30-15 is an ideal test candidate as a two component model has already been suggested to explain the spectral variability of this source (M<sup>c</sup>Hardy et al. 1998; Shih et al. 2002; Fabian & Vaughan 2003). We combine data from monitoring observations (Uttley et al., 2002) and a  $\sim 300$  ks long-look observation (Lee et al., 1999), all obtained during *RXTE* gain epoch 3. We extracted 256s-binned light curves for the entire data set in two energy bands, 2-5 keV (soft, channels 0-13) and 7-15 keV (hard, channels 19-41), using Standard 2 data from layer 1 of PCUs 0,1,2 and standard Good Time Interval selection criteria (Lamer et al., 2003). The latest L7 background models for faint sources were used to determine the background level for the PCA.

## 4 RESULTS

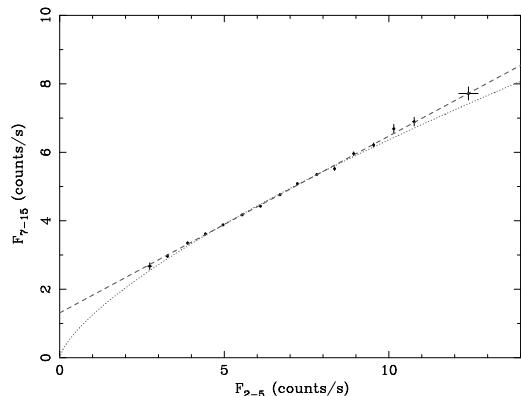
### 4.1 Flux-Flux plots

Using the 256s-binned hard and soft light curves, we made a flux-flux plot of the hard flux against the corresponding soft flux for each 256s segment (Fig. 2). A linear relationship between the soft and hard flux is apparent from visual examination of Figure 2. We next fitted a simple linear model,  $F_h = kF_s + C$ , to the data. We obtained fit parameters of  $k = 0.538$  and  $C = 1.170$  but the fit is poor (acceptance probability  $\ll 0.1\%$ ), due to significant scatter in the values of  $F_h$  for a given  $F_s$ . However, the scatter is small and contains no systematic deviations from a linear model, implying some weak spectral variability which is uncorrelated with flux.

The nature of the  $F_h$  vs  $F_s$  relationship can be seen with greater clarity by binning up the  $F_h$  vs  $F_s$  plot (Fig. 3). The linear model then provides a good fit to the data ( $\chi^2$  of 11.03 for 16 degrees of freedom) for fit parameters of  $k = 0.516 \pm 0.006$  and  $C = 1.312 \pm 0.038$ . We then fit the data with a simple power-law to determine whether the spectral variability may be caused by spectral pivoting of a single component in the absence of any other spectral components. The fit is not formally acceptable (rejected at  $P > 99.8\%$  confidence). Fit parameters of both linear and power-law model fits are summarised in Table 1. If a constant spectral component is included in the power-law fit (i.e. we fit the data with Equation 3) the fit converges to  $\alpha = 1$ , equivalent to

**Table 1.** Results of the linear and power-law fits to the flux-flux plots for each of the Seyfert galaxies in our sample.

Object	Linear model			Power-law model		
	$k_{lin}$	$C$	$\chi^2/\text{d.o.f.}$	$k_{pow}$	$\alpha$	$\chi^2/\text{d.o.f.}$
MCG–6-30-15	$0.516 \pm 0.006$	$1.310 \pm 0.036$	11.12/14	$1.251 \pm 0.030$	$0.707 \pm 0.013$	34.94/14
NGC 3516	$0.598 \pm 0.008$	$1.813 \pm 0.047$	13.45/14	$1.671 \pm 0.040$	$0.662 \pm 0.014$	36.98/14
NGC 5506	$0.822 \pm 0.022$	$1.429 \pm 0.126$	10.62/14	$1.369 \pm 0.070$	$0.850 \pm 0.020$	13.46/14
NGC 4051	$0.502 \pm 0.008$	$0.452 \pm 0.022$	63.18/11	$1.040 \pm 0.003$	$0.642 \pm 0.022$	22.95/11


**Figure 3.** The binned flux-flux plot for MCG–6-30-15. The dashed line represents the linear fit to the data and the dotted line the power-law fit (without a constant component).

the two-component linear model. The 90% confidence lower limit for  $\alpha$  using the power-law plus constant component model is 0.9. This value of  $\alpha$  corresponds to a pivot energy  $E_p > 10000$  keV which seems physically implausible since the high-energy cut-off in MCG–6-30-15 is at  $\sim 160$  keV (Guainazzi et al., 1999). We therefore reject the pivoting model for the spectral variability of MCG–6-30-15.

The linearity of the flux-flux relationship clearly implies a varying soft component with a spectral shape which is uncorrelated with flux (and which has a hardness ratio  $\sim 0.52$ ). A positive intercept on the hard flux axis, suggests the existence of a constant-flux component, which is harder than the varying component. We note that the hard component may be weakly varying, in order to provide the observed scatter in the unbinned flux-flux plot or, alternatively, the soft component may show variations in shape which are uncorrelated with flux. However, for simplicity we refer to these components as the soft varying component (SVC) and the hard constant component (HCC), which we identify with the components of the two-component models suggested by McHardy et al. (1998) and Shih et al. (2002), to explain the observed spectral variability of MCG–6-30-15. We will consider the specific spectral shapes of these components in Section 4.3.

## 4.2 Flux-Flux plots for other Seyferts

Having demonstrated that the two-component model for X-ray spectral variability is correct in the case of MCG–6-30-15, we now consider the spectral variability of some other Seyfert galaxies. We show binned-up flux-flux plots for NGC 5506, NGC 3516 and NGC 4051 in Fig. 4, made using *RXTE* monitoring data, in the same manner as the MCG–6-30-15 flux-flux plot (see Lamer et al.

2000, Lamer et al. 2003 and Uttley et al. 2002 for descriptions of the data). We fitted all the flux-flux plots with the linear two component model and the simple power-law model. The fit parameters are shown in Table 1 and the corresponding models plotting in Fig. 4. The NGC 3516 flux-flux plot is well fitted by a linear model, but a simple power-law is rejected by the data (at  $P > 99.9\%$  confidence). As in the case of MCG–6-30-15, the addition of a constant component to the power-law model yields a value of  $\alpha = 1$  (equivalent to the two-component model). At 90% confidence the lower limit for  $\alpha$  is 0.86, which corresponds to a pivot energy  $E_p > 3000$  keV. Hence we rule out spectral pivoting in the case of NGC 3516. Like MCG–6-30-15 the spectral variability in NGC 3516 results from two spectral components. The NGC 5506 flux-flux plot can be satisfactorily fitted by both the linear and power-law models. This ambiguity probably stems from the narrower flux range covered by the NGC 5506 data (which is a factor of two lower than seen in MCG–6-30-15 and NGC 3516). We note that the best fitting power-law index to the NGC 5506 flux-flux plot corresponds to a pivot energy  $E_p \sim 3000$  keV which again we consider unlikely.

A linear fit to the flux-flux plot for NGC 4051 can be rejected. The power-law model is a much better fit but is still rejected at  $P > 98\%$ , although we note that the pivot energy predicted by this model (around 50-60 keV) coincides with that estimated from the photon-index-flux correlation by Zdziarski et al. 2002). The addition of a constant component to the power-law results in a formally acceptable fit ( $\chi^2$  of 13.38 for 9 degrees of freedom), with fit parameters  $\alpha = 0.738^{+0.035}_{-0.055}$  (corresponding to pivot energy  $E_p \sim 300$  keV),  $k_{pow} = 0.838 \pm 0.104$  and  $C_h = 0.183 \pm 0.01$  for  $C_s = 0$ . A hard constant component appears to be required but the bulk of the spectral variability of NGC 4051 is a result of spectral pivoting.

## 4.3 The nature of the hard constant component

We have shown that there exist at least two modes of spectral variability in Seyfert galaxies: variability described by a simple linear two-component model where the soft component (SVC) varies in amplitude but not spectral shape, with respect to a hard component (HCC); and spectral variability where the varying component pivots, but a hard component is also present. In either case the hard component may be constant or weakly varying, but its flux is not correlated with the flux of the soft component. The SVC may simply understood as the varying power-law emission component (e.g. as measured using the ‘difference spectrum’, Fabian & Vaughan 2003). An interesting question is the nature and physical origin of the HCC. We now briefly investigate the shape of the HCC in the case of MCG–6-30-15, using information contained in the flux-flux plot.

As described in Section 2, the intercept on the hard flux axis of the flux-flux plot,  $C = C_h - kC_s$ , where  $C_h$  and  $C_s$  are the fluxes

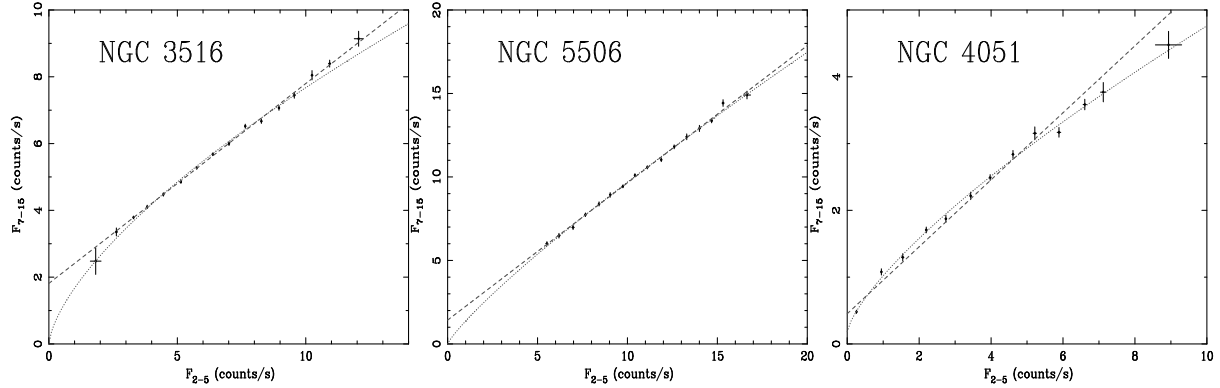


**Figure 4.** Binned flux-flux plots for NGC 5506, NGC 3516 and NGC 4051. The dashed lines represent linear fits to the data and the dotted line the power-law fits (without a constant component except in the case of NGC 4051 where we show the best fitting power-law plus constant model).

of the HCC in hard and soft bands respectively, and  $k$  is the hardness ratio of the SVC. In principle, one could measure many values of  $C$  from flux-flux plots for many energy bands, to create a set of simultaneous equations for the values of  $C$  which can be solved to yield the HCC flux in each band. However, the resulting equations (which we do not show here, but are simple to derive) are highly sensitive to the measured values of  $k$  and  $C$  so that even small uncertainties in the measured flux-flux relation make this method unfeasible. Instead, one can make a simple estimate of the shape of the HCC by making flux-flux plots in many bands and assuming the value of  $C_s$  in the softest band and then extrapolating the observed linear flux-flux relation to find the value of hard flux corresponding to that  $C_s$ .

To implement this method, we measured lightcurves in 10 narrow energy bands which do not overlap. The softest band covers the 2-4 keV range, seven bands of width  $\sim 1$  keV cover energies from 4-11 keV and two further bands cover 11-13 keV and 13-15 keV. We then made flux-flux plots for each of the bands above 4 keV versus the 2-4 keV band. All the flux-flux plots were well fitted by linear relations with intercepts on the hard flux axis. We chose 6 test values of the 2-4 keV HCC flux,  $C_s$ , in intervals of  $0.3 \text{ count s}^{-1}$  from  $C_s = 0 \text{ count s}^{-1}$  to  $C_s = 1.5 \text{ count s}^{-1}$  and determined the corresponding HCC flux in the other bands using the flux-flux relations (errors are calculated by propagating through the uncertainties in the linear fit parameters). In Fig. 5 we show the resulting family of HCC spectra, normalised relative to the total average spectrum, in order to show the shape of the HCC independent of the instrumental response. Note that the shape of the HCC above 4 keV is only weakly dependent on the assumed values of  $C_s$ , so the method appears to be quite robust in constraining the HCC shape. It can be seen that the HCC is significantly harder than the total spectrum. Furthermore, a prominent feature can be seen around 6-7 keV, suggesting that the HCC contains stronger iron features than are seen in the total spectrum.

A simple interpretation of the HCC is that it corresponds to reflection of the SVC from distant cold material (perhaps the putative molecular torus), and hence can remain constant despite large changes in the illuminating continuum flux. However, we note that even the minimum possible contribution of the HCC (corresponding to  $C_s = 0$ ) exceeds 30% of the total flux at 10 keV, significantly larger than the  $< 10\%$  of total flux expected for reflection from cold material which covers half the sky as seen from the continuum source (see Fig. 5 and George & Fabian 1991; Magdziarz &

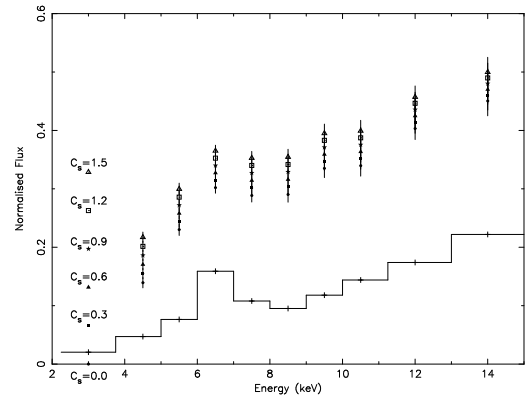


**Figure 5.** Estimated HCC spectra normalised by the total average spectrum (see 4.3 for details). Also plotted as a stepped line is the expected maximal reflection spectrum (including a narrow iron  $K\alpha$  line) for cold distant material which covers half the sky as seen from the continuum source (assuming solar abundances and reflector inclination angle of  $0^\circ$ ).

Zdziarski 1995). We will examine the shape of the HCC in more detail, and in other AGN, in a future paper, but for now we concur with the interpretation of Fabian & Vaughan (2003) that the HCC may represent reflection from the inner disk which is boosted by light-bending effects close to a rapidly rotating black hole (although how such a component remains constant is not yet clear, but see Fabian & Vaughan 2003 for further discussion).

## 5 DISCUSSION

We have introduced the flux-flux plot as a model independent technique for distinguishing between two modes of spectral variability in Seyfert galaxy spectra; pivoting of a single spectral component or changes in the relative normalisation of a constant hard and varying soft component with constant spectral shape (the two-component model). We have shown that the two-component model is correct for MCG-6-30-15 and NGC 3516 but the pivoting model applies in NGC 4051 (albeit with an additional constant hard component). The data for NGC 5506 is less clear cut and does not allow a definitive conclusion as to the nature of the spectral variability in this AGN, probably due to the smaller flux range sampled by the data.

This ambiguity in the nature of the flux-flux plot can be avoided by comparing fluxes in more widely separated hard and soft bands, so that the index of the power-law flux-flux plot expected from pivoting is decreased (due to the greater relative change in the hard and soft fluxes). *XMM-Newton* observations should be able to provide the necessary separation of the hard and soft energy bands that is required, to distinguish the two possibilities in NGC 5506 and similar cases.

It is interesting that both pivoting and constant-shape modes of spectral variability are seen in the black hole candidate Cyg X-1 (Zdziarski et al., 2002) with pivoting being observed in the hard state only and a constant spectral shape seen in both hard and soft states. Zdziarski et al. (2002) review how these different types of spectral variability can result from a two-phase disk-corona model, where the accretion disk illuminates the hot corona with low energy seed photons to produce the hard X-ray emission via inverse Compton scattering (e.g. Haardt & Maraschi 1993), which in turn feeds back to affect the seed photon emission by heating the disk. For example, spectral pivoting results when the luminosity of the corona (which dissipates most of the gravitational energy release) is kept constant, while the seed photon luminosity varies. Spectral pivoting may also be produced if the corona is pair dominated. A constant spectral shape (as in the case of the two-component model) is produced when the total luminosity of both disk and corona increases. Zdziarski et al. (2002) suggest that changes in the seed photon luminosity or total luminosity may correspond, respectively, to a reduction in disk inner radius (so the corona sees more of the disk emission) or an increase in accretion rate. However, it is not clear how these physical models can explain the very rapid spectral variations in AGN, where most of the flux variations (and corresponding spectral changes) occur on short time-scales (hours to days), much shorter than the expected viscous time-scales in these objects.

Applying the AGN/X-ray binary analogy suggested by the remarkably similar variability properties of these objects (e.g. Uttley et al. 2002), one might think that the spectral pivoting observed for NGC 4051 implies that this AGN occupies the hard state, corresponding to a low accretion rate (few per cent of Eddington). However, the X-ray timing properties (power spectrum) of NGC 4051 show a strong similarity to the soft state of Cyg X-1 (M<sup>c</sup>Hardy et al., 2003, in prep), and the low mass of this AGN suggests a high accretion rate of a few tens of per cent or larger (Shemmer et al. 2003, M<sup>c</sup>Hardy et al., 2003, in prep.). The power spectrum and spectral-timing properties (coherence, phase lags) of NGC 4051 M<sup>c</sup>Hardy et al. (2003, in prep.), are also similar to those of MCG–6-30-15 (Vaughan et al., 2003), despite the apparently different spectral variability modes operating in these AGN.

One apparent difference between NGC 4051 and MCG–6-30-15 is that NGC 4051 shows a significantly larger variability amplitude (by about a factor 2) than MCG–6-30-15, on all time-scales. It is difficult to see how such a large variability amplitude (especially on short time-scales) could be caused by variations in the seed photon flux. However, if the seed photon luminosity is dominated by internal viscous heating in the disk (i.e. X-ray heating is not significant) *but* the corona dissipates most of the accretion power, then a relatively small change in dissipation rate in the corona, if fed back to the disk, could result in a large change in the seed photon luminosity and relatively little change in coronal (and total) luminosity, thus satisfying the conditions for spectral pivoting. Different dissipation mechanisms, and different coupling strengths between disk and corona could then result in the different spectral variability modes that we see. The similar power spectral shape and spectral-

timing properties observed in MCG–6-30-15 and NGC 4051 may indicate that these properties are linked to the more general properties of the corona (e.g. radial distribution of emission, temperature gradient) rather than the disk-corona coupling mechanism (e.g. see Kotov et al. 2001 for a possible model which can explain these timing properties).

Finally, we note that the hard, constant component in the spectrum of MCG–6-30-15 appears to be broadly consistent with a pure reflection spectrum but the strength of this component suggests that the reflection is somehow boosted, perhaps by relativistic beaming and gravitational light bending effects (Martocchia et al., 2000). Such a scenario can be realised if the reflector lies close to a central Kerr black hole, as also suggested by Fabian & Vaughan (2003) who describe how such a model might explain the constancy of the reflection spectrum despite large changes in the soft component flux.

### Acknowledgments

We wish to thank Simon Vaughan for valuable comments and discussions. This research has made use of data obtained from the High Energy Astrophysics Science Archive Research Center (HEASARC), provided by NASA's Goddard Space Flight Center.

This paper has been produced using the Royal Astronomical Society/Blackwell Science L<sup>A</sup>T<sub>E</sub>X style file.

### References

- Chiang J., Reynolds C. S., Blaes O. M., Nowak M. A., Murray N., Madejski G., Marshall H. L., Magdziarz P., 2000, *ApJ*, 528, 292
- Churazov E., Gilfanov M., Revnivtsev M., 2001, *MNRAS*, 321, 759
- Done C., Madejski G. M., Życki P. T., 2000, *ApJ*, 536, 213
- Fabian A. C., Vaughan S., 2003, *MNRAS*, pp astro-ph/0301588
- George I. M., Fabian A. C., 1991, *MNRAS*, 249, 352
- Green A., M<sup>c</sup>Hardy I., Lehto H., 1993, *MNRAS*, 265, 664
- Guainazzi M., Matt G., Molendi S., Orr A., Fiore F., Grandi P., Matteuzzi A., Mineo T., Perola G. C., Parmar A. N., Piro L., 1999, *A&A Lett.*, 341, L27
- Haardt F., Maraschi L., 1993, *ApJ*, 413, 507
- Haardt F., Maraschi L., Ghisellini G., 1997, *ApJ*, 476, 620
- Iwasawa K., Fabian A. C., Reynolds C. S., Nandra K., Otani C., Inoue H., Hayashida K., Brandt W. N., Dotani T., Kunieda H., Matsuoka M., Tanaka Y., 1996, *MNRAS*, 282, 1038
- Kotov O., Churazov E., Gilfanov M., 2001, *MNRAS*, 327, 799
- Lamer G., M<sup>c</sup>Hardy I., Uttley P., Jahoda K., 2003, *MNRAS*, 338, 323
- Lamer G., Uttley P., M<sup>c</sup>Hardy I., 2000, *MNRAS*, 319, 949
- Lee J. C., Fabian A. C., Brandt W. N., Reynolds C. S., Iwasawa K., 1999, *MNRAS*, 310, 973
- Lee J. C., Fabian A. C., Reynolds C. S., Brandt W. N., Iwasawa K., 2000, *MNRAS*, 318, 857
- Magdziarz P., Zdziarski A. A., 1995, *MNRAS*, 273, 837
- Martocchia A., Karas V., Matt G., 2000, *MNRAS*, 312, 817
- M<sup>c</sup>Hardy I., Papadakis I., Uttley P., 1998, *Nucl. Phys. B (Proc. Suppl.)*, 69/1-3, 509
- Shemmer O., Uttley P., Netzer H., M<sup>c</sup>Hardy I. M., 2003, *MNRAS*, pp astro-ph/0209363
- Shih D. C., Iwasawa K., Fabian A. C., 2002, *MNRAS*, 333, 687

## 6 *Taylor, Uttley & McHardy*

Uttley P., McHardy I. M., Papadakis I. E., 2002, MNRAS, 332, 231

Vaughan S., Fabian A. C., Nandra K., 2003, MNRAS, 339, 1237

Zdziarski A. A., Gilfanov M., Lubinski P., Revnivtev M., 2003, MNRAS, pp astro-ph/0209363

Zdziarski A. A., Poutanen J., Paciesas W. S., Wen L., 2002, ApJ, 578, 357